ANALYTICAL HIERARCHY PROCESS FOR LANDSLIDE SUSCEPTIBILITY MAPPING IN LOWER MAE CHAEM WATERSHED, NORTHERN THAILAND

Narumon Intarawichian*[*] and Songkot Dasananda

Received: Apr 26, 2010; Revised: Jul 13, 2010; Accepted: Aug 2, 2010

Abstract

Landslide hazard results in great loss of life and property. These damages can be mitigated if the cause and effect relationships of the events are known. In this study, we used analytical hierarchy process (AHP) and weighted linear combination (WLC) methods to produce landslide susceptibility map of the lower Mae Chaem Watershed in the north of Thailand. The study was carried out using remote sensing data, field surveys and geographic information system (GIS) tools. The ten factors that influence landslide occurrence, such as elevation, slope aspect, slope angle, distance from drainage, lithology, distance from lineament, soil texture, precipitation, land use/land cover (LULC) and NDVI were considered. The landslide susceptibility index (LSI) was calculated using the WLC technique based on the assigned weight and rating given by the AHP method. The result of analysis was verified using existing landslide locations where the accuracy rate of 64.90% was accomplished. The obtained landslide susceptibility map is useful for landslide hazard prevention and mitigation, and proper planning for land use and construction in the future.

Keywords: Landslide susceptibility, analytical hierarchy process, GIS, remote sensing

Introduction

Landslides are destructive natural phenomena that frequently lead to serious problems in hilly regions, resulting in loss of human life and property and severe damage to natural resources. Risk from landslide is normally defined as the expected number of lives lost, persons injured, property damages and disrupted economic activities due to a particular landslide hazard for a given area and reference period (Varnes, 1984). To reduce risk from the landslide incidences, knowledge of the areas potentially prone to landslide activity is crucially needed. This information is typically described in the form of landslide susceptibility map for the interested area. Formulation of this map depends on complex knowledge of slope movements and their controlling factors.

Reliability of the susceptibility maps depends mostly on the amount and quality of available data, the working scale and the selection of the appropriate methodology of

School of Remote Sensing, Institute of Science, Suranaree University of Technology, Nakhon Ratchasima, 30000, Thailand. E-mail: narumon_intara@yahoo.com
[*] *Corresponding author*

analysis and modeling. The process of creating the maps involves several qualitative or quantitative approaches (e.g., Soeters and Van Westen, 1996; Aleotti and Chowdhury, 1999; Guzzetti *et al*., 1999). Early attempts had defined susceptibility classes by qualitative overlaying of geological and morphological slope-attributes to landslide inventories (Nielsen *et al*., 1979). However, more sophisticated assessments involved techniques such as AHP, bivariate, multivariate, logistics regression, fuzzy logic, or artificial neural network (ANN) have been reported in recent years. For examples; by Chacón *et al*. (2006); Lee *et al*. (2006); Lee and Pradhan (2006, 2007); Lee (2007a and b); Akgun and Bulut (2007); Akgun *et al*. (2008); Oh *et al*. (2008); Muthu *et al*. (2008); Van Westen *et al*. (2008); Vijith and Madhu (2008) and Pradhan and Lee (2009).

Qualitative methods depend critically on expert opinions. Most common types simply examine landside inventory maps to identify sites of similar geological and geomorphological properties that are likely susceptible to failure. Some qualitative approaches, however, incorporate the idea of ranking and weighting, and may evolve to be semi-quantitative in nature. The application of the analytical hierarchy process (AHP) method, developed by Saaty (1980), for landslide susceptibility mapping has been found in, e.g., Barredo *et al*. (2000); Mwasi (2001); Nie *et al*. (2001) and Yagi (2003), while the use of weighted linear combination (WLC) technique was reported in Ayalew *et al*. (2004). Being partly subjective, results of these approaches vary depending on knowledge of experts. Hence, qualitative or semi-quantitative methods are often useful for regional studies (Soeters and Van Westen, 1996; Guzzetti *et al*., 1999).

Quantitative methods are based on numerical expressions of the relationship between controlling factors and landslide activity. There are two types of quantitative methods: deterministic and statistical (Aleotti and Chowdhury, 1999). Deterministic quantitative methods depend on engineering principles of slope instability expressed in terms of the factor of safety. Due to the need for exhaustive data from individual slopes, these methods are often effective for mapping only small areas. Landslide susceptibility mapping using either multivariate or bivariate statistical approaches analyzes the historical link between landslide-controlling factors and the distribution of landslides (Guzzetti *et al*., 1999).

The increase of computer-based tools has been found to be useful in the hazard mapping of landslides. One of such significant tools is geographic information systems (GIS). A GIS is commonly defined as a powerful set of tools for collecting, storing, retrieving at will, displaying, and transforming spatial data (Burrough and McDonnel, 1998). With help of GIS, it is possible to integrate spatial data of different layers to determine influence of the parameters on landslide occurrence. The process of GIS-aided landslide susceptibility mapping at present involves several methods that can be considered as either qualitative or quantitative as stated earlier.

Study Area

The lower Mae Chaem watershed is a significant basin of Mae Ping River, which is the main river in the upper north Thailand and the largest tributary of central Thailand's Chao Phraya River. Its location is approximately at latitudes 18°06′00″N to 18°38′24″N and longitudes 98°04′12″E to 98°38′24″E, covering area of about 1,932 km^2 in the Chiang Mai and Mae Hong Son Provinces. It comprises of 3 districts (or Amphoe) within Chiang Mai border and two districts within Mae Hong Son border.

Topography of the watershed is relatively steep with elevation ranging from 260 m to 2540 m, and small narrow floodplains appear close to the river (Figure 1). About 90% of its area is mountainous covered with diversified plant communities that form various types of forest, where rice and other agricultural products, especially vegetables and orchards, are normally cultivated in the low area. In recent years, the watershed has experienced several devatated landslide incidences that brought vast damage to properties and natural environment, and some loss of human life (Table 1).

Based on field surveys and local records, the dominant landslides found in the area are shallow slides on steep slopes, especially those associated with the granite

Table 1. Summary of the crucial landslide incidences in the study area

Date/Place	The effect of the disaster
September 15, 2002 Mae Chaem, Chiang Mai	The infrastructures were affected such as bridge, road, drainage systems and agricultural areas.
October 2, 2002 Mae Sariang, Mae Hong Son	The infrastructures were affected such as bridge, road, drainage systems and agricultural areas with several casualties.
May 6, 2004 Mae Chaem, Chiang Mai	1 people died, 3 houses were destroyed, agricultural areas and property were affected.
September 14, 2005 Mae Sariang and Mae La Noi, Mae Hong Son	The infrastructures were affected such as bridge, road.
September 19, 2005 Mae Chaem, Chiang Mai	Some houses were destroyed, and infrastructures were affected such as bridge, road, drainage systems and agricultural areas.

Source : Department of Mineral Resources, Mae Chaem District Office and internet resource)

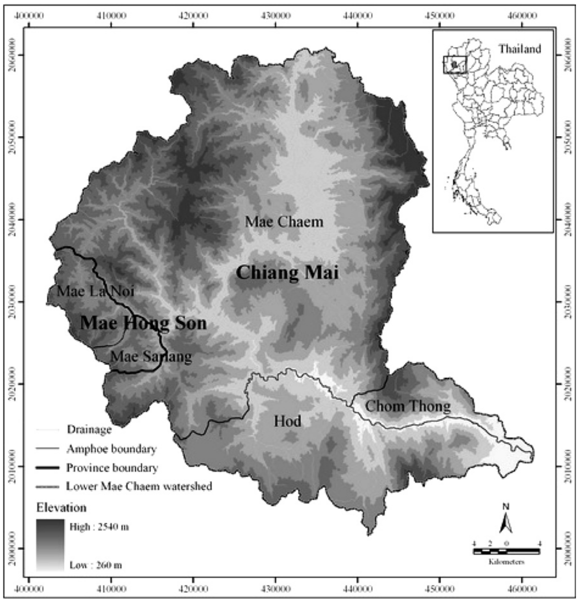

Figure 1. Location map of the study area, the lower Mae Chaem watershed

terrain, being triggered by the prolonged heavy rainfall. However, rock falls and deep seated failures have also been found infrequently.

Data and Methodology

Data

Typically, the instability factors that can introduce severe landslides in some particular area include surface and bedrock, lithology and structure, seismicity, slope, steepness, morphology, stream evolution, groundwater conditions, climate, vegetation cover, land use, and human activity. In this study, ten factors were considered which are elevation, slope aspect, slope angle, distance from drainage, lithology, distance from lineament, soil texture, rainfall, land use/land cover (LULC) and the normalized difference vegetation index (NDVI). The first eight factors were extracted from the associated database acquired from the respective responsible agencies (as detailed in Table 2), while LULC and NDVI maps were derived from the Landsat-5 TM satellite images (Tables 2 and Figures 2(a-j)). These factors can be separated into three broad categories: geological, topographical and environmental conditioning parameters. The working scale of geographic maps was chosen at 1:50,000. All the collected data were converted to a raster grid with 25 m × 25 m cells for the use with AHP technique. The total cell number is 3091791 for this study.

The first three components (elevation, slope aspect, slope angle) were derived from digital elevation model (DEM) of the study area at 10-meter contour interval using the

Table 2. Spatial data layers used in the study

Category	Layer	Data type	Scale	Data source
Topographic map	Elevation	Point and line	1:50,000	Royal Thai Survey Department
	Slope aspect			
	Slope angle			
Drainage map	Distance from drainage	Polygon	1:50,000	
Geological map	Lithology	Polygon	1:50,000	Department of Mineral Resources
Lineament map	Distance from lineament	Polygon	1:50,000	
Soil map	Soil texture	Polygon	1:50,000	Land Development Department
Precipitation map	Precipitation	GRID	1:50,000	1. Thai Meteorological Department 2. The GAME-T project
LULC map	Land use/land cover	GRID	25 m × 25 m	Derivation from Landsat-5 TM images (taken on 12 February 2001 and 26 February 2006)
NDVI map	NDVI	GRID	25 m × 25 m	

appropriate commands in ArcGIS's Surface Analyst tools. Slope aspect was determined by the down-slope direction of the maximum rate of change in value from each cell to its neighbors. Final results were reported in terms of the 8 basic compass directions on the output map (Figure 2(c)).

Slope angle identifies the steepest downhill slope for a location on a surface that can be calculated for each triangle in TIN and for each cell in raster. For a TIN, this is the maximum rate of change in elevation across each triangle. For raster, it is the maximum rate of change in elevation over each cell and its eight neighbors. The slope angle command takes an input surface raster and calculates an output raster containing the slope angle at each cell. The lower the slope angle value, the flatter the terrain; the higher the slope angle value, the steeper the terrain. The output slope angle raster can be calculated as percent slope angle or degree of slope angle.

In addition, distance from drainage was found using the topographic database. The drainage buffer was calculated at 100-meter intervals. The lithology map was prepared from a 1:50,000 scale geological map. The distance from lineament was calculated in 100-meter intervals. The soil texture was prepared from 1:50,000 scale soil map. The precipitation data were provided by the Thai Meteorological Department (TMD) and the GAME-T project over the period of the study, and the kriging interpolation method was used to produce rainfall intensity map of the area.

LULC data were generated from Landsat-5 TM images using an unsupervised classification method (ISODATA) and field surveys where twelve classes; which are paddy field, mixed field crop, longan, truck crop, mixed swidden cultivation, hill evergreen forest, mixed deciduous forest, mixed forest plantation, grass and scrub, mine, urban, and water, were identified for LULC mapping (Figure 2(i)).

Finally, the NDVI map was generated from Landsat-5 TM satellite images (resolution of 25 m). The NDVI involves a non-linear transformation of the visible or red and near-infrared bands of satellite images (Rouse *et al*., 1973; Jackson *et al*., 1983; Tucker *et al*., 1991). It can be calculated using formula

$$NDVI = (NIR-R)/(NIR+R) \quad (1)$$

where NIR and R are the observed reflectance in the near infrared and red portions of the electromagnetic spectrum, respectively. NDVI can be regarded as a rough measure of vegetation amount in terms of biomass, leaf area index (LAI), and percentage of vegetation cover. Its values range from -1 to +1 (pixel values 0–255).

Methodology

In this study, the AHP technique was used to produce landslide susceptibility map for the lower Mae Chaem watershed, which is being one of the well-known landslide hotspots in northern Thailand. To achieve this, the relevant thematic layers pertaining causative factors were generated using remotely-sensed data, field surveys and GIS tools. Landslide susceptibility map of the study area was eventually prepared using AHP method. In this method, the landslide susceptibility index (LSI) value for each considered pixel was computed by summation of each factor's weight multiplied by class weight (or rating) of each referred factor (for that pixel) written as follows::

$$LSI = \sum_{i=1}^{n} (W_i \times R_i) \quad (2)$$

where LSI is the required landslide susceptibility index of the given pixel, R_i and W_i are class weight (or rating value) and the factor weight for factor i derived using AHP technique (Table 4). All found LSI values were then separated into five classes using natural breaks algorithm to represent five categories of the landslide susceptibility zone (LSZ) of the area; namely, 1. very high (VHS), 2. high (HS), 3. moderate (MS), 4. low (LS) and 5. very low (VLS) susceptibility zones (Table 5). Finally, validity of the map was examined using 25 known landslide locations within the area obtained from the field surveys and from official records of the responsible authorities.

Analytical Hierarchy Process (AHP)

AHP involves building a hierarchy of decision elements (factors) and then making comparisons between possible pairs in a matrix to give a weight for each element and also a consistency ratio. It is based on three principles: decomposition, comparative judgment and synthesis of priorities (Malczewski, 1999). WLC is a standard concept to combine maps of landslide-controlling parameters by applying a standardized score (primary-level weight) to each class of a certain parameter

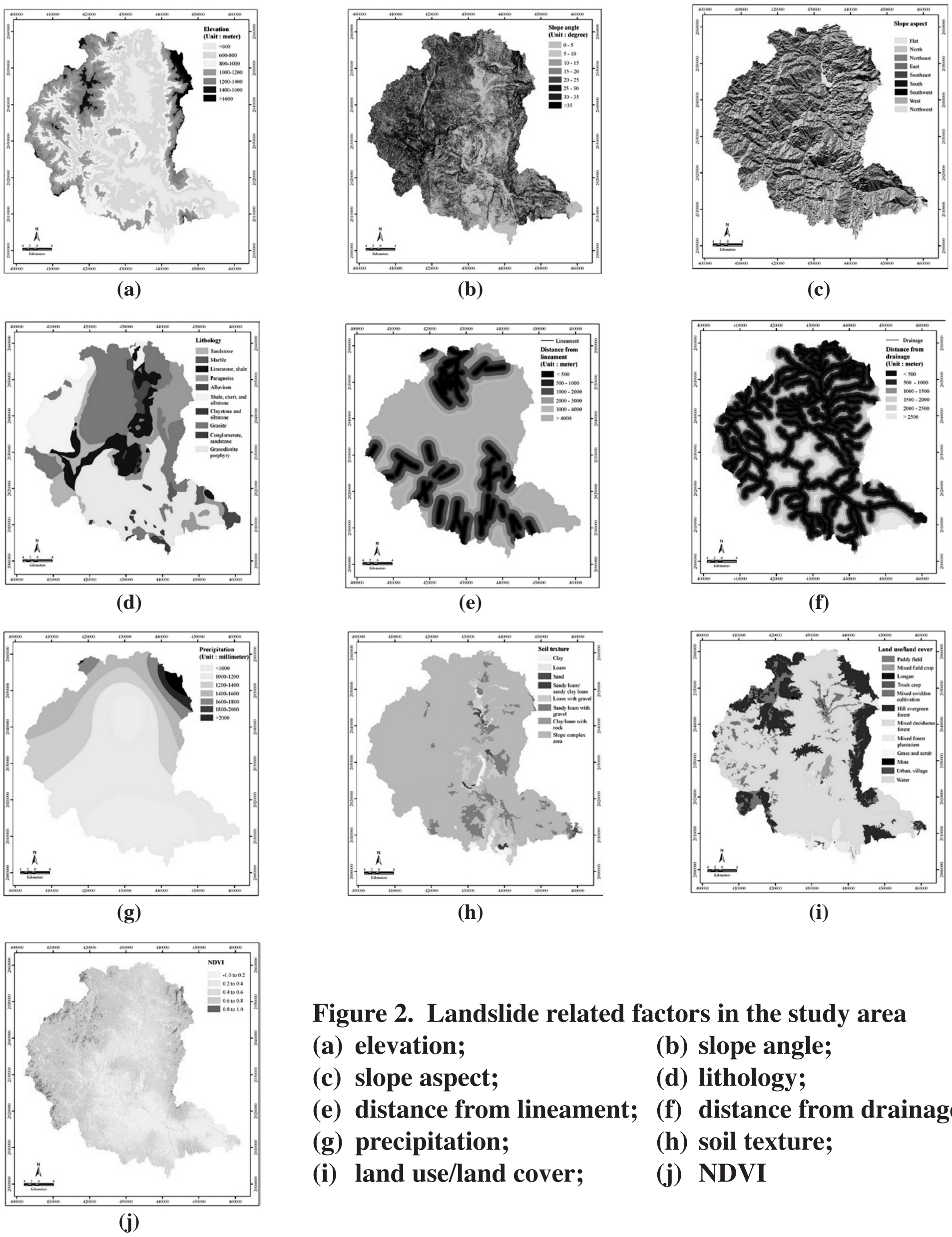

(a) (b) (c) (d) (e) (f) (g) (h) (i) (j)

Figure 2. Landslide related factors in the study area
(a) elevation; (b) slope angle; (c) slope aspect; (d) lithology; (e) distance from lineament; (f) distance from drainage; (g) precipitation; (h) soil texture; (i) land use/land cover; (j) NDVI

and a factor weight (secondary-level weight) to the parameters themselves.

Analytical hierarchy process (AHP) is a semi-qualitative method, which involves a matrix-based pair-wise comparison of the contribution of different factors for landsliding. It was developed by Saaty (1980) and gained widespread attention later on. Factor weights for each criterion are determined by a pair-wise comparison matrix as described by Saaty (1990, 1994), and Saaty and Vargas (2001). To get factor weights in AHP, one has to build a pair-wise comparison matrix with scores given in Table 3. In the construction of a pair-wise comparison matrix, each factor is rated against every other factor by assigning a relative dominant value between 1 and 9 to the intersecting cell. When the factor on the vertical axis is more important than the factor on the horizontal axis, this value varies between 1 and 9. Conversely, the value varies between the reciprocals 1/2 and 1/9. Since we have used ten parameters, the comparison matrix has 100 boxes. However, because the pair-wise comparison matrices are symmetrical in nature, only 55 values were needed to fill in the diagonal and the lower triangular half of the matrix. Then, in order to compute the principal eigenvector of the matrix and obtain a best-fit set of factor weights automatically as suggested by Saaty (1994) and Saaty and Vargas (2001), raster maps produced by combining the parameters with landslide distribution were necessary.

In this study, AHP considers weighting and rating system developed by collecting questionnaires from expert opinions and concerned research organizations, such as the Department of Mineral Resources and the Land Development Department, and the selection of the appropriate criteria and scores was guided by 20 experts from various Thai government officials. The diagonal boxes of a pair-wise comparison matrix always take a certain value of 1. The boxes in the upper and lower halves are symmetrical with one another and the corresponding values are, therefore, reciprocal with each other. Once the matrix is constructed, weights whose sum equals one, will be obtained by computer based image processor with thematic layers of all causal factors categorized on the basis of class weights as inputs. But, when the parameters are few, weights can also be derived by a series of simple summation and division processes. The weights are then

Table 3. Scale of preference between two parameters in AHP (Saaty, 2000)

Scales	Degree of preferences	Explanation
1	Equally	Two activities contribute equally to the objective.
3	Moderately	Experience and judgment slightly to moderately favor one activity over another.
5	Strongly	Experience and judgment strongly or essentially favor one activity over another.
7	Very strongly	An activity is strongly favored over another and its dominance is showed in practice.
9	Extremely	The evidence of favoring one activity over another is of the highest degree possible of an affirmation.
2, 4, 6, 8	Intermediate values	Used to represent compromises between the preferences in weights 1, 3, 5, 7 and 9.
Reciprocals	Opposites	Used for inverse comparison.

considered as the average of all possible ways of comparing the causal factors (Malczewski, 1999).

Application of AHP

The final result consists of the derived factor weights and class weights, and a calculated consistency ratio (CR), as seen in Table 4. In AHP, the consistency used to build a matrix is checked by a consistency ratio, which depends on the number of parameters. For a 10×10 matrix, the CR must be less than 0.1 to accept the computed weights. The CR is a ratio between the matrix's consistency index and random index, and in general ranges from 0 to 1. The random index is the average consistence index obtained by generating large numbers of random matrices. A CR close to 0 indicates the high probability that the weights were generated randomly (Saaty, 1980; 1994).

The models with a CR greater than 0.1 were automatically rejected, while a CR less than 0.1 were often acceptable. With the AHP method, the values of spatial factors weights were defined. Using a weighted linear sum procedure (Voogd, 1983), the acquired weights were used to calculate the landslide susceptibility. In this study, the CR is 0.068, the ratio indicates a reasonable level of consistency in the pair-wise comparison, that is good enough to recognize the factor weights. Consequently, the weight corresponding to precipitation is highest, whereas elevation is lowest (Table 4). For all cases of the gained class weights, the CRs less than 0.1, the ratio indicates a reasonable level of consistency in the pair-wise comparison that was good enough to recognize the class weights.

Results and Discussion

Using the AHP, the LSI values were computed by using Equation (2). From the calculation, it was found that the LSI had a minimum value of 0.04, and a maximum value of 0.28, with an average value of 0.11 and a standard deviation of 0.03. The LSI represents the relative susceptibility of a landslide occurrence. Therefore, the higher the index, the more susceptible the area is to landslide. These LSI values were then divided into five classes based on the natural breaks range, which represent five different zones in the landslide susceptibility map. These are very high (VHS), high (HS), moderate (MS), low (LS) and very low (VLS) susceptibility zones (Figure 3). The percentage covering areas of each susceptibility class are shown in Table 5 along with number of reference landslide points occurred.

From data seen in Table 5, it is obvious that only 23.35% of the total area were classified as being in the VHS (5.51%) or HS (17.84%) landslide susceptibility zones but they had accommodated about 60% of the landslide reference points. Other areas are located in the MS (28.47%), LS (29.32%), and VLS (18.86%) susceptibility zones and only 1 landslide incidence (out of 25) being observed in the LS and VLS zones. To evaluate validity of the results shown in Table 5 more quantitatively, the frequency ratio (FR) values for each identified class are also given. These values were computed from ratio of the percentage landslide occurrences and the percentage area coverage (for each individual class to the whole study area). The possible values begin from 0 onwards where relatively high ones (e.g. much greater than 1) indicate high chance of having landslides while low values (e.g. close to 0) indicate lower chance of having landslide over the area. FR equals 1 means the considered area is having equal chance for landslide occurrence to that of the average value for the entire area. The FR values of 4.36 for the VHS zone and 2.02 for the HS zone indicate the notably higher chance of having landslide activities in these areas when compared to those of the MS (1.26) and LS (0.14).These results emphasize the applicability of the susceptibility map that was constructed based on the AHP method and being depicted in Figure 3.

Verification of the Result

Finally, the resulted susceptibility map produced was verified based on known 25 landslide locations located within the study area where the area under curve (AUC)

Table 4. The pair-wise comparison matrix, factor weights, class weights (rating) and consistency ratio

Factors	1	2	3	4	5	6	7	8	9	10	11	12	Rating
Elevation (m)													
(1) <600	1												0.027
(2) 600 – 800	2	1											0.037
(3) 800 - 1,000	3	2	1										0.059
(4) 1,000 - 1,200	4	3	2	1									0.087
(5) 1,200 – 1,400	5	4	3	2	1								0.126
(6) 1,400 – 1,600	7	6	5	4	3	1							0.239
(7) >1,600	9	8	7	6	5	3	1						0.426
Consistency ratio: 0.040													
Slope aspect													
(1) Flat	1												0.026
(2) North	3	1											0.071
(3) Northeast	5	3	1										0.189
(4) East	3	1	1/3	1									0.071
(5) Southeast	3	1	1/3	1	1								0.071
(6) South	3	1	1/3	1	1	1							0.071
(7) Southwest	7	5	3	5	5	5	1						0.354
(8) West	3	1	1/3	1	1	1	1/5	1					0.071
(9) Northwest	3	1	1/3	1	1	1	1/5	1	1				0.071
Consistency ratio: 0.008													
Slope angle													
(1) 0º – 5º	1												0.024
(2) 5º – 10º	2	1											0.031
(3) 10º – 15º	3	2	1										0.048
(4) 15º – 20º	4	3	2	1									0.069
(5) 20º – 25º	5	4	3	2	1								0.103
(6) 25º – 30º	6	5	4	3	2	1							0.146
(7) 30º – 35º	7	6	5	4	3	2	1						0.205
(8) >35º	9	8	7	6	5	4	3	1					0.378
Consistency ratio: 0.037													
Drainage (m)													
(Distance from drainage)													
(1) <500	1												0.462
(2) 500 – 1,000	1/3	1											0.255
(3) 1,000 – 1,500	1/5	1/3	1										0.138
(4) 1,500 – 2,000	1/7	1/5	1/3	1									0.067
(5) 2,000 – 2,500	1/8	1/6	1/4	1/2	1								0.048
(6) >2,500	1/9	1/7	1/5	1/3	1/2	1							0.032
Consistency ratio: 0.045													

Table 4. (Continued)

Factors	1	2	3	4	5	6	7	8	9	10	11	12	Rating
Lithology													
(1) Sandstone	1												0.124
(2) Marble	1/3	1											0.053
(3) Limestone, shale	1/3	1	1										0.053
(4) Paragneiss	1/2	2	2	1									0.083
(5) Alluvium	1/5	1/3	1/3	1/4	1								0.024
(6) Shale, chert, and siltstone	1/3	1	1	1/2	3	1							0.053
(7) Claystone and siltstone	1/4	1/2	1/2	1/3	2	1/2	1						0.031
(8) Granite	3	5	5	4	7	5	6	1					0.273
(9) Conglomerate, sandstone	1	3	3	2	5	3	4	1/3	1				0.124
(10) Granodiorite porphyry	2	4	4	3	6	4	5	1/2	2	1			0.187
Consistency ratio: 0.017													
Lineament (m) (Distance from lineament)													
(1) <500	1												0.293
(2) 500 – 1,000	1	1											0.293
(3) 1,000 – 2,000	1/2	1/2	1										0.177
(4) 2,000 – 3,000	1/3	1/3	1/2	1									0.107
(5) 3,000 – 4,000	1/4	1/4	1/3	1/2	1								0.067
(6) >4,000	1/4	1/4	1/3	1/2	1	1							0.067
Consistency ratio: 0.008													
Soil texture													
(1) Clay	1												0.019
(2) Loam	4	1											0.055
(3) Sand	8	5	1										0.238
(4) Sandy loam / sandy clay loam	7	4	1/2	1									0.169
(5) Loam with gravel	5	2	1/4	1/3	1								0.086
(6) Sandy loam with gravel	9	6	2	3	5	1							0.335
(7) Clay/loam with rock	3	1/2	1/6	1/5	1/3	1/7	1						0.039
(8) Slope complex area	4	1	1/5	1/4	1/2	1/6	2	1					0.055
Consistency ratio: 0.034													

Table 4. (Continued)

Factors	1	2	3	4	5	6	7	8	9	10	11	12	Rating
Precipitation (mm)													
(1) <1,000	1												0.027
(2) 1,000 – 1,200	2	1											0.036
(3) 1,200 – 1,400	3	2	1										0.053
(4) 1,400 – 1,600	5	4	3	1									0.103
(5) 1,600 – 1,800	6	5	4	2	1								0.143
(6) 1,800 – 2,000	8	7	6	4	3	1							0.266
(7) >2,000	9	8	7	5	4	2	1						0.376
Consistency ratio: 0.049													
Land use/land cover													
(1) Paddy field	1												0.137
(2) Mixed field crop	1/2	1											0.090
(3) Longan	1/3	1/2	1										0.063
(4) Truck crop	1/2	1	2	1									0.090
(5) Mixed swidden cultivation	1/2	1	2	1	1								0.090
(6) Hill evergreen forest	1/7	1/6	1/5	1/6	1/6	1							0.017
(7) Mixed deciduous forest	1/6	1/5	1/4	1/5	1/5	2	1						0.023
(8) Mixed forest plantation	1/5	1/4	1/3	1/4	1/4	3	2	1					0.033
(9) Grass and scrub	1/4	1/3	1/2	1/3	1/3	4	3	2	1				0.045
(10) Mine	2	3	4	3	3	8	7	6	5	1			0.200
(11) Urban, village	2	3	4	3	3	8	7	6	5	1	1		0.200
(12) Water	1/8	1/7	1/6	1/7	1/4	1/2	1/3	1/4	1/5	1/9	1/9	1	0.013
Consistency ratio: 0.039													
NDVI													
(1) -1.0 to 0.2	1												0.502
(2) 0.2 to 0.4	1/3	1											0.256
(3) 0.4 to 0.6	1/5	1/3	1										0.120
(4) 0.6 to 0.8	1/6	1/4	1/2	1									0.074
(5) 0.8 to 1.0	1/7	1/5	1/3	1/2	1								0.050
Consistency ratio: 0.031													

Table 4. (Continued)

Data layers	1	2	3	4	5	6	7	8	9	10	11	12	Weights
Elevation	1												0.027
Slope aspect	1	1											0.030
Slope angle	5	4	1										0.165
Drainage	2	1/2	1/5	1									0.034
Lithology	5	5	2	3	1								0.170
Lineaments	3	5	1/2	4	1/2	1							0.121
Soil texture	2	3	1/5	3	1/2	1/3	1						0.054
Precipitation	5	6	2	5	3	3	5	1					0.259
Land use	4	4	1/3	3	1/4	1/3	3	1/5	1				0.082
NDVI	3	3	1/5	2	1/5	1/4	2	1/5	1/2	1			0.057
Consistency ratio: 0.068													

Table 5. Allocation of the reference landslide points within the defined landslide susceptibility classes and the associated frequency ratio (FR) of each class

Susceptibility classes	Susceptibility index values	% of Area	Number of landslide points	Frequency ratio (FR)
Very low susceptibility (VLS)	0.04 – 0.08	18.86	- (0%)	0.0
Low susceptibility (LS)	0.08 – 0.11	29.32	1 (4%)	0.1364
Moderate susceptibility (MS)	0.11 – 0.13	28.47	9 (36%)	1.2645
High susceptibility (HS)	0.13 – 0.16	17.84	9 (36%)	2.0179
Very high susceptibility (VHS)	0.16 – 0.28	5.51	6 (24%)	4.3557

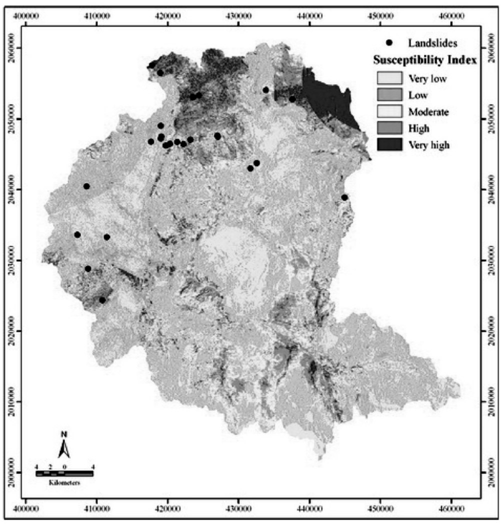

Figure 3. The landslide susceptibility map based on AHP with 25 known landslide locations on the basis of natural breaks classification

method (as described in Lee *et al*., 2004) was used. In this method, the computed index values (LSI) of all cells within the study area (3,091,791 cells in this case) were sorted in descending order (from high to low values of LSI). Then these ordered cell values were divided into 100 classes, with accumulated 1% intervals. This resulted in 100 landslide susceptibility classes available for performing the accuracy assessment (instead of just only 5 classes as listed in Table 5). The ranking orders (from 1 to 100) were then given to each class beginning from the very high susceptibility ones (VHS) towards the very low susceptibility ones (VLS), respectively.

To assess the predictive capability of the map quantitatively, the LSI ranking orders (1-100) were plotted against accumulative amount of landslide incidences for each specific class (given in term of percentage of the total number). This appears as a line seen in Figure 4. This result indicates that the first 20% of the area that LSI has highest rank (VHS zone) could explain 24% of all the referred landslides. In addition, the first 30% of the total area where the LSI had a higher rank could explain 36% of the total landslides. Then, the prediction accuracy of the map can be readily evaluated from the area under the plotting curve (AUC) by assuming that perfect prediction will have maximum AUC of 1. In our study (Figure 4), the AUC was found to be 0.6490. As a result, it could state that the prediction accuracy of the obtained map is 64.90% with respect to the ideal value of 100%, which is fairly satisfied.

Although, the prediction accuracy of the map is not considerably high, it can still be regarded as being promising tool for responsible authorities in planning proper prevention and mitigation strategies related to landslide incidences in the noted landslide prone areas on the map. The priority should be given to the areas that locate within the VHS and HS zones as they are most likely to have landslide activity if the triggering factors (especially prolonged heavy rainfall) are experienced. Therefore, the effective warning system should be established at some mostly concerned areas. And close monitoring of the improper landuse activities and permanent human settlements should be taken care of by the responsible authorities to reduce possible damages due to severe landslides in the VHS and HS zones of the study area in the future.

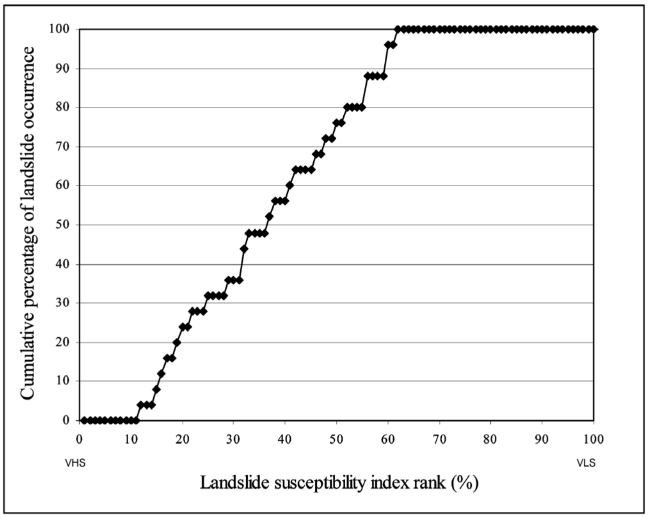

Figure 4. Illustration of cumulative frequency diagram showing landslide susceptibility index rank (x-axis) occurring in cumulative percent of landslide occurrence (y-axis)

Conclusions

In this study, the analytical hierarchy process (AHP) was applied to develop landslide susceptibility map for the lower Mae Chaem watershed located in northern Thailand. To achieve this objective, ten landslide inducing factors were taken into consideration, which are elevation, slope aspect, slope angle, distance from drainage, lithology, distance from lineament, soil texture, precipitation, land use/land cover (LULC) and NDVI. The first eight parameters were extracted and calculated from their associated database (Table 2) while LULC and NDVI maps were derived from Landsat-5 TM satellite images. These factors were evaluated, then factor weight and class weight were assigned to each of the associated factors.

Based on the results given in Table 4, the three most influencing factors to landslide activity (judged from their associated weights) are precipitation (0.259), lithology (0.17), and slope angle (0.165). And the three least influencing factors are elevation (0.027), slope aspect (0.03), and distance from drainage (0.034). The obtained susceptibility map and its relevant data (Figure 3 and Table 5) indicate that the high and very high susceptible zones cover about 23.35% of the total area while about 48.18% were classified as being the low and very low susceptible zones. The map was verified using existing landslide location data based on the area under curve (AUC) method from which the prediction accuracy of 64.90% was accomplished.

Acknowledgements

The authors are grateful to the support of the Geo-Informatics and Space Technology Development Agency (GISTDA) for providing the Landsat-5 TM satellite images of the study area. Special thanks are due to the Mae Chaem District officers and staffs for providing valuable background information on the landslide activity over the study area and the help in the field surveys. This research was supported by grants from the Commission on Higher Education, the Ministry of Education of Thailand. Valuable comments and suggestions on the original manuscript from two anonymous reviewers are also appreciated.

References

Akgun, A. and Bulut, F. (2007). GIS-based landslide susceptibility for Arsin-Yomra (Trabzon, North Turkey) region. Environ Geol, 51(8):1377–1387.

Akgun, A., Dag, S., and Bulut, F. (2008). Landslide susceptibility mapping for a landslide-prone area (Findikli, NE of Turkey) by likelihood-frequency ratio and weighted linear combination models. Environ Geol, 54:1127-1143.

Aleotti, P. and Chowdhury, R. (1999). Landslide hazard assessment: summary review and new perspectives. Bulletin of Engineering Geology and the Environment, 58:21–44.

Ayalew, L., Yamagishi, H., and Ugawa, N. (2004). Landslide susceptibility mapping using GIS-based weighted linear combination, the case in Tsugawa area of Agano River, Niigata Prefecture, Japan. Landslides, 1:73–81.

Barredo, J.I., Benavidesz, A., Herhl, J., and Van Westen, C.J. (2000). Comparing heuristic landslide hazard assessment techniques using GIS in the Tirajana basin, Gran Canaria Island, Spain. JAG, 2:9–23.

Burrough, P.A. and McDonnel, R. (1998). Principles of Geographical Information Systems. 2nd ed. Oxford University Press, London, 193p.

Chàcon, J., Irigaray, C., Fernàndez, T., and El Hamdouni, R., (2006). Engineering geology maps: landslides and geographical information systems. Bulletin of Engineering Geology and the Environment, 65:341–411.

GISTDA. (2009). Thailand's first Observation Satellite, THEOS (in Thai). Geo-Informatics and Space Technology Development Agency (Public Organization): GISTDA [On-line]. Available: http://

theos.gistda.or.th

Guzzetti, F., Carrarra, A., Cardinali, M., and Reichenbach, P. (1999). Landslide hazard evaluation: a review of current techniques and their application in a multi-scale study, Central Italy. Geomorphology, 31:181–216.

Lee, S. (2007a). Application and verification of fuzzy algebraic operators to landslide susceptibility mapping. Environmental Geology, 52(4):615–623.

Lee, S. (2007b). Comparison of landslide susceptibility maps generated through multiple logistic regression for three test areas in Korea. Earth Surface Processes and Landforms. 32:2133–2148.

Lee, S. and Pradhan, B. (2006). Landslide hazard assessment at Cameron Highland Malaysia using frequency ratio and logistic regression models. Geophy Res Abstracts, 8:SRef-ID:1607–7962/gra/EGU06-A-03241.

Lee, S. and Pradhan, B. (2007). Landslide hazard mapping at Selangor, Malaysia using frequency ratio and logistic regression models. Landslides, 4(1):33–41.

Lee, S., Choi, J., and Min, K. (2004). Probabilistic landslide hazard mapping using GIS and remote sensing data at Boun, Korea. Int J Remote Sens, 25:2037–2052.

Lee, S., Ryu, J.H., Lee, M.J., and Won, J.S. (2006). The application of artificial neural networks to landslide susceptibility mapping at Janghung, Korea. Math Geol, 38(2):199–220.

Malczewski, J. (1999). GIS and Multi-Criteria Decision Analysis. 1st ed. John Wiley and Sons, NY, 392p.

Muthu, K., Petrou, M., Tarantino, C., and Blonda, P. (2008). Landslide Possibility Mapping Using Fuzzy Approaches. IEEE Transactions on Geoscience and Remote Sensing, 46(4):1253–1265.

Mwasi, B. (2001). Land use conflicts resolution in a fragile ecosystem using Multi-Criteria Evaluation (MCE) and a GIS-based Decision Support System (DSS). Proceedings of the International Conference on Spatial Information for Sustainable Development; October 2-5, 2001; FIG-International Federation of Surveyors; Nairobi, Kenya, p. 11.

Nie, H.F., Diao, S.J., Liu, J.X., and Huang, H. (2001). The application of remote sensing technique and AHP-fuzzy method in comprehensive analysis and assessment for regional stability of Chongqing City, China. Proceedings of the 22nd International Asian Conference on Remote Sensing; November 5-9, 2001; University of Singapore, Singapore, 1:660–665.

Nielsen, T.H., Wrigth, R.h., Vlasic, T.C., and Spangle, W.E. (1979). Relative slope stability and land-use planning in the San Francisco Bay region, California. US Geological Survey Professional p. 944.

Oh, H.J., Lee, S., Chotikasathein, W., Kim, C.H., and Kwon, J.H. (2008). Predictive landslide susceptibility mapping using spatial information in the Pechabun area of Thailand. Environ Geol, 43:120–131.

Pradhan, B. and Lee, S. (2009). Landslide risk analysis using artificial neural network model focussing on different training sites. Int. J. Phy. Sci., 4(1):1-15.

Saaty, T.L. (1980). The Analytical Hierarchy Process. McGraw Hill, NY, 350p.

Saaty, T.L. (1990). The Analytic Hierarchy Process: Planning, Priority Setting, Resource Allocation. 1st ed. RWS Publications, Pittsburgh, 502p.

Saaty, T.L. (1994). Fundamentals of Decision Making and Priority Theory with Analytic Hierarchy Process. 1st ed. RWS Publications, Pittsburgh, 527p.

Saaty, T.L. and Vargas, L.G. (2001). Models, Methods, Concepts, and Applications of the Analytic Hierarchy Process. 1st ed. Kluwer Academic, Boston, 333p.

Soeters, R. and Van Westen, C.J. (1996). Slope stability: recognition, analysis and zonation. In: Landslides: Investigation and Mitigation. Turner, A.K. and Shuster, R.L. (eds.). Transportation research Board–National Research Council. Special Report 247, p. 129–177.

Van Westen, C.J., Castellanos Abella, E.A., and Sekhar, L.K. (2008). Spatial data for landslide susceptibility, hazards and vulnerability assessment: an overview. Eng Geol, 102(3-4):112-131.

Varnes, D.J. (1984). Landslide Hazard Zonation: a Review of Principles and Practice. Natural Hazards. No. 3. 1st ed. UNESCO, Paris, France, 63p.

Vijith, H. and Madhu, G. (2008). Estimating potential landslide sites of an upland sub-watershed in Western Ghat's of Kerala (India) through frequency ratio and GIS. Environ Geol, 55:1397-1405.

Voogd, H. (1983). Multicriteria Evaluation for Urban and Regional Planning. 1st ed. Pion Ltd., London, 367p.

Yagi, H. (2003). Development of assessment method for landslide hazardness by AHP. Abstract Volume of the 42nd Annual Meeting of the Japan Landslide Society, p. 209–212.